

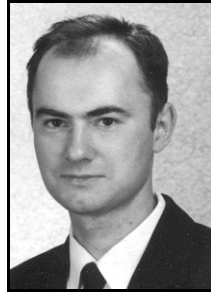
Sławomir KARYŚ

KIELCE UNIVERSITY OF TECHNOLOGY, POWER ELECTRONIC DEPARTMENT

Phase-Shift Driven Class D Series Resonant Inverter With Two Anti Parallel-Connected Auxiliary Switches

Ph.D. Sławomir KARYŚ

Sławomir Karyś was born in Kielce, Poland, in 1966. He received the MSc and Ph.D. degrees from Kielce University of Technology, in 1991 and 2001, respectively. The main fields of his scientific interest are high power resonant inverters for electric or hybrid vehicles.



e-mail: enesk@tu.kielce.pl

Abstract

This paper presents analysis of a novel voltage source class D inverter. The classic topology has been extended of the two auxiliary switches, that are anti parallel connected and each of them has its own resonant inductor. Proposed solution enables phase-shift control of the inverter, keeping zero-current-switching for auxiliary transistors. This paper explains the operation principle that is illustrated by simulation, presents general equations, design and shows experimental results.

Keywords: soft switching, ZCS, phase-shift control, class D inverter.

Sterowany fazowo przekształtnik rezonansowy klasy D z dwoma łącznikami połączonymi odwrotnie równolegle

Streszczenie

W artykule zaprezentowano analizę nowego rozwiązania przekształtnika klasy D, zasilanego ze źródła napięcia. Układ klasycznego przekształtnika został rozszerzony o dwa dodatkowe klucze, które są połączone przeciw równolegle i posiadają własne indukcyjności stanowiące elementy obwodu rezonansowego. Zaproponowane rozwiązanie umożliwia sterowanie fazowe przekształtnika, przy zachowaniu wyłączenia tranzystorów pomocniczych w warunkach zerowego prądu – ZCS. Artykuł przedstawia podstawowe równania, budowę i wyniki badań eksperymentalnych przekształtnika.

Słowa kluczowe: miękkie przełączanie, ZCS, sterowanie fazowe, przekształtnik klasy D.

1. Introduction

Class D resonant inverters are widely used to convert dc energy into ac energy. The main field of the applications are electronic ballast for fluorescent lamps, induction-heating process [1]. The circuit of the modified class D inverter with two anti parallel auxiliary switches is shown in Fig. 1.1.

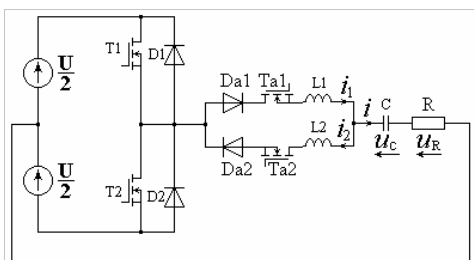


Fig. 1.1. The class D inverter with two anti parallel auxiliary switches
Rys. 1.1. Przekształtnik Klasy D z dwoma łącznikami pomocniczymi połączonymi przeciw równolegle

The two additional transistors Ta1, Ta2, diodes Da1, Da2 and resonant inductors L1, L2, enable phase shift control of the inverter. In the past, the idea with two separated inductors has been used for phase-controlled rectifiers [2, 3]. Nowadays this solution can be introduced in the soft switching inverter to simplify output power control.

The paper explains the operation principle, then it shows simulation analyses. In the end experimental results are presented.

2. Operation Principle of the Inverter

The main transistors T1 and T2 are switched with constant duty cycle 50% and constant basic frequency f slightly higher than resonant frequency f_o . Load current is delayed in refer to the first harmonic of the output voltage. The auxiliary transistors Ta1, Ta2 have their own resonant inductors L1 and L2. The auxiliary transistors are controlled by phase shift signals that are referred to the basic frequency f . The inverter can be driven in a wide range of the turn on delay angle ϑ_{on} - from 0 to π . According to the angle ϑ_{on} of the control signal for auxiliary transistors, the load current can be continuous or discontinuous. The most complex waveforms of the load current are shown in Fig. 2.1.

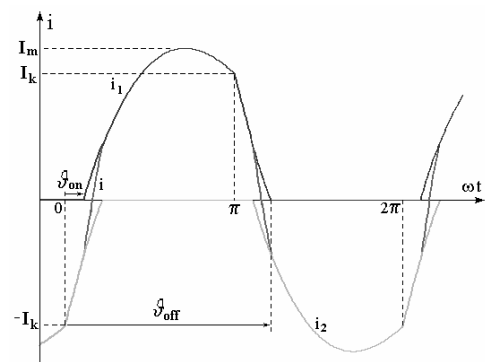


Fig. 2.1. Waveforms of the load current i and resonant inductor current i_1, i_2

Rys. 2.1. Prąd obciążenia i oraz prądy rezonansowe w indukcyjnościach i_1, i_2

The analysis is carried out under following assumptions:

- transistors and diodes are ideal devices (with zero on resistance, infinite off resistance, zero threshold voltage),
- inverter is fed by an ideal dc voltage source,
- elements of the series-resonant circuit are passive, linear and time invariant.

Inductor current i_1 is given by

$$\text{for } \vartheta_{on} \leq \varphi \leq \pi \quad i_1 = I_m e^{-\frac{ak\varphi}{\omega}} \sin k(\varphi - \vartheta_{on}) \quad (2.1)$$

$$\text{for } \pi < \varphi \leq \vartheta_{off} \quad i_1 = \left(I_m - \frac{U}{\omega_R L}\right) e^{-\frac{ak\varphi}{\omega}} \sin k(\varphi - \pi) + I_k \quad (2.2)$$

where

$$L_1 = L_2 = L, \quad \varphi = \omega t, \quad \omega = 2\pi f, \quad k = \frac{\omega_R}{\omega}, \quad \omega_R^2 = \omega_0^2 - \alpha^2,$$

$$\omega_0 = \frac{1}{\sqrt{LC}}, \alpha = \frac{R}{2L}, I_m = \frac{U - 2U_0}{2\omega_R L}, I_k = I_m e^{\frac{\alpha k \pi}{\omega}} \sin k(\pi - \vartheta_{on}),$$

$$U_0 \approx \omega_0 L I_m e^{\frac{\alpha k \pi}{\omega}} \sin k(\pi - \vartheta_{on})$$

Similar equations can be obtained for the inductor current i_2 . For $(\vartheta_{on} < \varphi \leq \vartheta_{off} - \pi)$ the load current flows through both inductors and is given by

$$i = i_1 - i_2 = \frac{U}{\omega_R L} e^{\frac{\alpha k \varphi}{\omega}} \sin k(\varphi - \vartheta_{on}) - I_k \quad (2.3)$$

From Fig. 2.1 it can be seen that out of the regions $(\vartheta_{on}, \vartheta_{off} - \pi)$ and $(\pi + \vartheta_{on}, \vartheta_{off})$, the load current is equal to i_1 or i_2 .

The output power for discontinuous current region $(\vartheta_{off} - \vartheta_{on} < \pi)$ is given by

$$P = \frac{U}{2k} \left(1 + \frac{\alpha^2}{\omega_R^2}\right)^{-1} \left\{ I_m e^{\frac{\alpha k \vartheta_{on}}{\omega}} \left(\cos k \vartheta_{on} + \frac{\alpha}{\omega_R} \sin k \vartheta_{on} \right) - \left(2I_m - \frac{U}{\omega_R L} \right) e^{\frac{\alpha k \pi}{\omega}} \left(\cos k \pi + \frac{\alpha}{\omega_R} \sin k \pi \right) \right\} + \left(I_m - \frac{U}{\omega_R L} \right) e^{\frac{\alpha k \vartheta_{off}}{\omega}} \left(\cos(k \vartheta_{off}) + \frac{\alpha}{\omega_R} \sin(k \vartheta_{off}) \right) - \frac{I_k U}{2} (\vartheta_{off} - \pi) \quad (2.4)$$

And for continuous current region $(\vartheta_{off} - \vartheta_{on} \geq \pi)$, the output power can be described by

$$P = \frac{U}{2k} \left(1 + \frac{\alpha^2}{\omega_R^2}\right)^{-1} \left\{ I_m e^{\frac{\alpha k \vartheta_{on}}{\omega}} \left(\cos k \vartheta_{on} + \frac{\alpha}{\omega_R} \sin k \vartheta_{on} \right) + \left(I_m - \frac{U}{\omega_R L} \right) e^{\frac{\alpha k \vartheta_{off}}{\omega}} \left(\cos(k \vartheta_{off} - \pi) + \frac{\alpha}{\omega_R} \sin(k \vartheta_{off} - \pi) \right) \right\} + e^{\frac{\alpha k \vartheta_{on}}{\omega}} \left(\cos(k \pi + \vartheta_{on}) + \frac{\alpha}{\omega_R} \sin(k \pi + \vartheta_{on}) \right) - \left(2I_m - \frac{U}{\omega_R L} \right) e^{\frac{\alpha k \pi}{\omega}} \left(\cos k \pi + \frac{\alpha}{\omega_R} \sin k \pi \right) - \frac{3U I_k}{4} (\vartheta_{off} - \pi - \vartheta_{on}) \quad (2.5)$$

Both equations (2.4) and (2.5) show that output power is a nonlinear function of the turn on delay angle ϑ_{on} .

3. Simulations Results

Simulation analysis has been made by means of TCAD program. The simulation circuit is shown in Fig. 3.1 [4]. To simplify the control of the inverter model, the auxiliary devices have been replaced by thyristors.

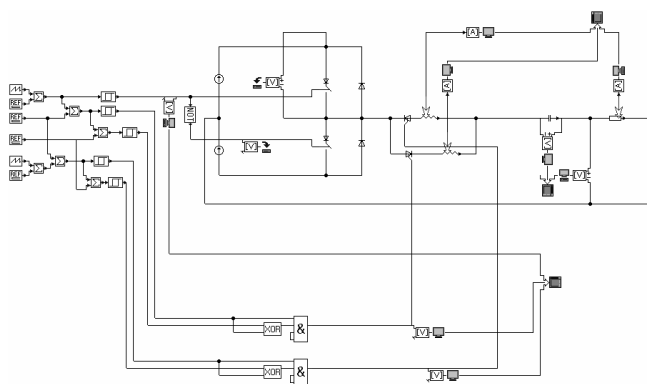


Fig. 3.1. Simulation circuit
Rys. 3.1. Model symulacyjny

The waveforms below have been computed under following assumptions: $f = 360$ kHz, $R = 10 \Omega$, $L_1 = L_2 = 9 \mu\text{H}$, $C = 47$ nF, $f_0 = 245$ kHz.

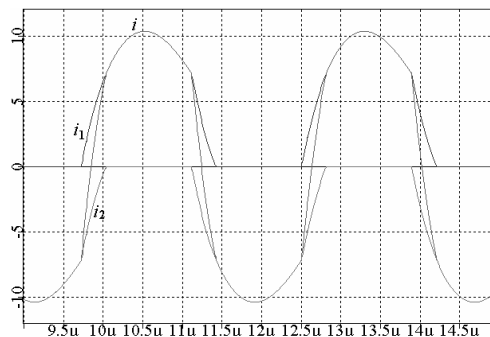


Fig. 3.2. Currents: i_1, i_2, i for $\vartheta_{on} = 0$
Rys. 3.2. Prądy: i_1, i_2, i dla $\vartheta_{on} = 0$

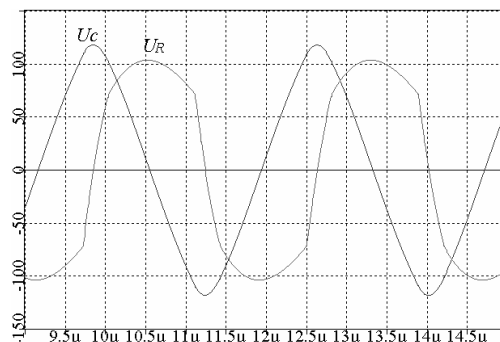


Fig. 3.3. Voltages: U_C, U_R for $\vartheta_{on} = 0$
Rys. 3.3. Napięcia: U_C, U_R dla $\vartheta_{on} = 0$

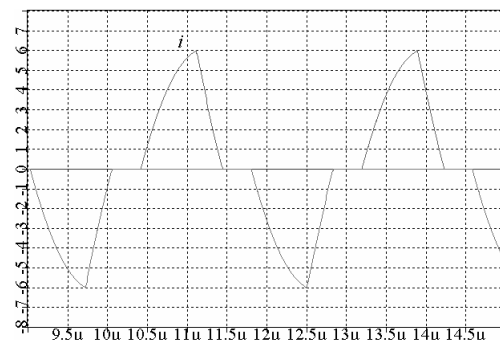


Fig. 3.4. Currents: i_1, i_2, i for $\vartheta_{on} = \frac{\pi}{2}$
Rys. 3.4. Prądy: i_1, i_2, i dla $\vartheta_{on} = \frac{\pi}{2}$

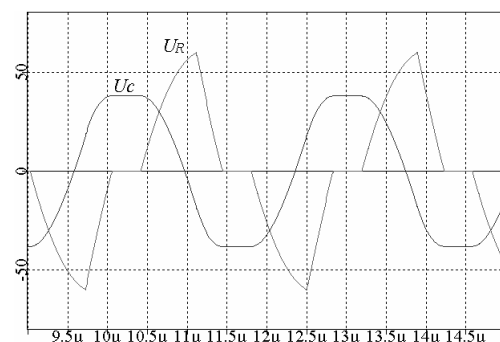


Fig. 3.5. Voltages: U_C, U_R for $\vartheta_{on} = \frac{\pi}{2}$
Rys. 3.5. Napięcia: U_C, U_R dla $\vartheta_{on} = \frac{\pi}{2}$

When the turn on delay angle ϑ_{on} is less than $\vartheta_{off} - \pi$, the load current is continuous.

The output power plots family versus the angle ϑ_{on} (in degrees) for the simulated inverter are shown in Fig. 3.6.

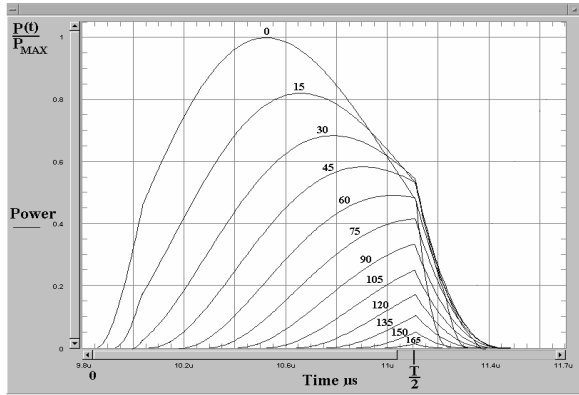


Fig. 3.6. Output power in function of the delay angle ϑ_{on}
 Rys. 3.6. Moc wyjściowa w funkcji kąta opóźnienia wysterowania ϑ_{on}

4. Experimental Results

The 200 W model of the resonant converter was build and experimental investigations were made. The converter consist of the power unit and control unit. The main devices in power unit are IRFPE50 Power Mosfet transistors and HFA16TB60 fast diodes. Transistors are driven from phase shift control unit through gate transformers. Fig. 4.1 shows driving signals for main transistor T1 and corresponding auxiliary transistor Ta1.



Fig. 4.1. Driving signals for main transistor T1 – CH3 (upper) and auxiliary transistor Ta1 – CH4 (lower): a) $\vartheta_{on} = \pi$, b) $\vartheta_{on} = \frac{\pi}{3}$
 Rys. 4.1. Sygnał sterujący tranzystor główny T1 – CH3 (górnny) oraz tranzystor pomocniczy Ta1 – CH4 (dolny): a) $\vartheta_{on} = \pi$, b) $\vartheta_{on} = \frac{\pi}{3}$

Fig. 4.2 shows waveforms of the load current and resonant capacitor voltage for following parameters: $U=40$ V, $f = 96$ kHz, $R = 6,5 \Omega$, $L_1 = L_2 = 110 \mu\text{H}$, $C = 28$ nF, $f_0 = 90,7$ kHz.

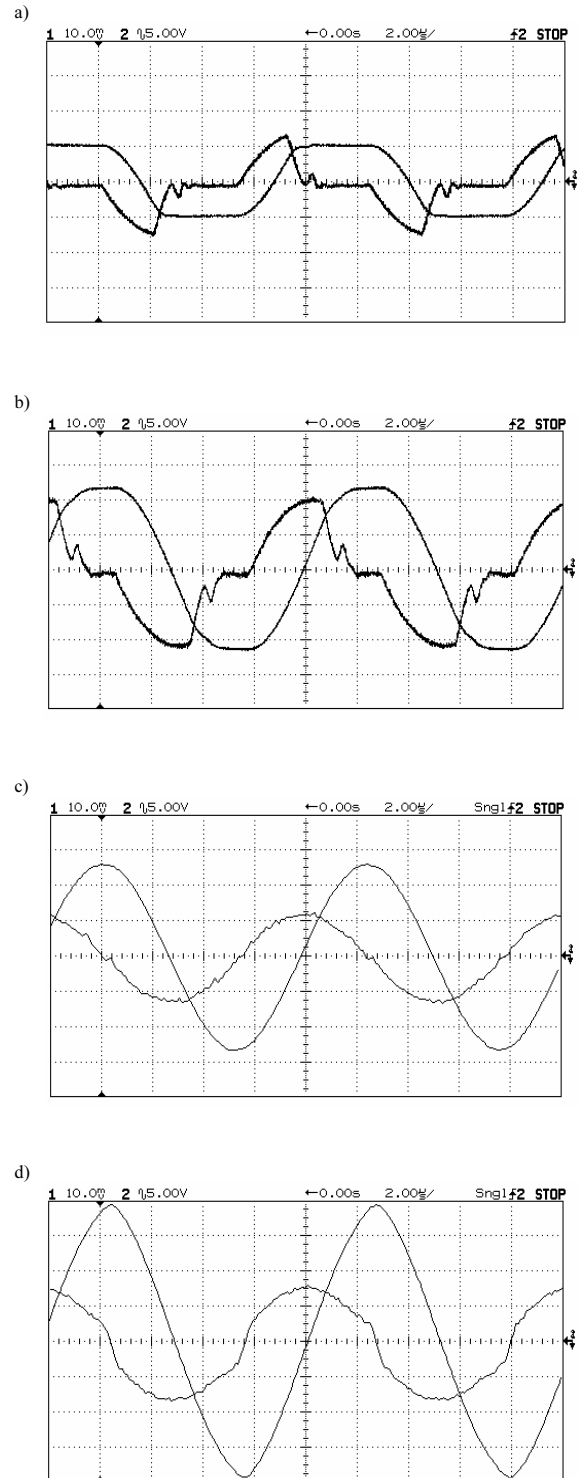


Fig. 4.2. Load current (0,5A/div) and resonant capacitor voltage waveforms for:
 a) $\vartheta_{on} = 2\pi/3$, b) $\vartheta_{on} = \pi/2$, c) $\vartheta_{on} = 0$, d) $\vartheta_{on} = -\pi/6$
 Rys. 4.2. Prąd obciążenia (0,5A/div) oraz napięcie na kondensatorze rezonansowym dla: a) $\vartheta_{on} = 2\pi/3$, b) $\vartheta_{on} = \pi/2$, c) $\vartheta_{on} = 0$, d) $\vartheta_{on} = -\pi/6$

It can be seen from above waveforms, that the current and therefore the output power is controlled by delay angle ϑ_{on} . Fig. 4.2 d) shows what happens, when the control system produces the angle ϑ_{on} less than zero - the auxiliary transistors are hard switched. Whenever main transistors are switched there are

transient spikes appearing in the current waveforms. This additional current follows through the parasitic capacitors of the main and auxiliary power elements that are serially connected.

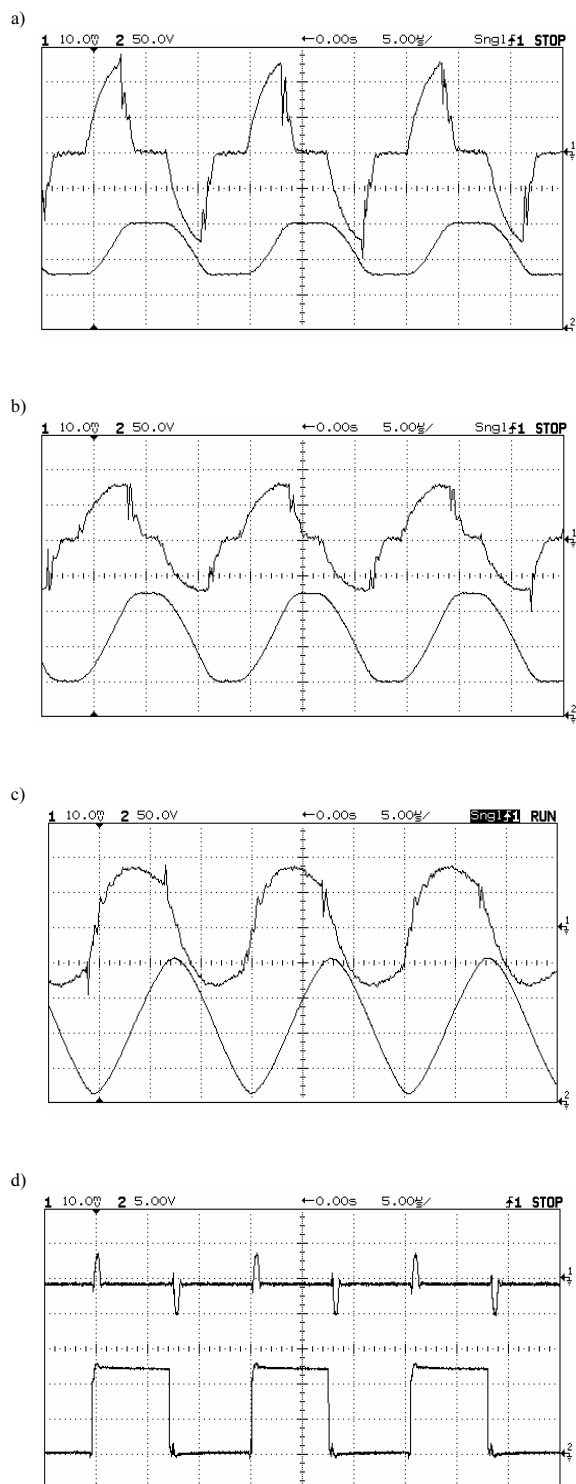


Fig. 4.3. Load current (2A/div) and resonant capacitor voltage waveforms for: a) $\vartheta_{on} = 2\pi/3$, b) $\vartheta_{on} = \pi/2$, c) $\vartheta_{on} = 0$. d) Current spikes (0,2A/div) and driving signal $\vartheta_{on} = \pi$,

Rys. 4.3. Prąd obciążenia (2A/div) oraz napięcie na kondensatorze rezonansowym dla: a) $\vartheta_{on} = 2\pi/3$, b) $\vartheta_{on} = \pi/2$, c) $\vartheta_{on} = 0$. d) Impulsy prądowe (0,2A/div) oraz sygnał sterujący dla $\vartheta_{on} = \pi$

Fig. 4.3 shows the load current and resonant capacitor voltage for nominal supply voltage $U=240\text{ V}$ and $f=67\text{ kHz}$, $R=25,5\ \Omega$, $L_1=L_2=110\ \mu\text{H}$, $C=58\ \text{nF}$, $f_0=63\ \text{kHz}$.

It can be seen from Fig. 4.3 d), that when the main transistor T1 is switched on or off, current spikes equal to 0,15A appear in the output current. At higher output power rates, this interferences can be neglected.

5. Conclusions

This paper presents a novel phase shift driven class D inverter. The shown solution is far different from the well known full bridge phase shift class D inverters [5]. The introduced innovation is based on two separated resonant inductors, which enable simple phase shift control of the inverter. Output power is easy regulated by turn on delay angle ϑ_{on} . Classic control method - simple [6] or modified [7] pulse density modulation has limited range of the output power regulation and wide EMI noise spectrum. In the developed inverter the load current is continuous when the turn on delay angle $\vartheta_{on} \leq \vartheta_{off} - \pi$. Considering the simulation and

experimental results, the load current is continuous if $\vartheta_{on} \leq \frac{\pi}{4}$.

Simple and low cost control system based on phase shift waveforms has been used. Timing requirements for control signals are not critical. Auxiliary transistors are switched at ZCS conditions. The inverter has low switching losses at delay angle ϑ_{on} near zero. At high angle ϑ_{on} , the main transistors are hard switched. Therefore this converter should be turned on with angle ϑ_{on} equal to π (zero output power) and smoothly go to angle near to zero (full power). Power semiconductors for this converter must have very small parasitic capacitance.

6. References

- [1] M. K. Kazimierczuk, D. Czarkowski.: „Resonant Power Converter” John & Sons, Inc. Canada 1995.
- [2] H. Tunia, B. Winiarski.: *Energoelektronika*, WNT, Warszawa 1996.
- [3] H. Tunia, H. Supronowicz.: *Sterownik tyrystorowy do regulacji prądu indukcyjnego*, Patent, Politechnika Warszawska 111447/191444/1976-07-27/1978-01-30 1980-08/30/-/H02P 13/4.
- [4] S. Karyś.: *Szeregowy falownik rezonansowy klasy D sterowany fazowo z dwoma łącznikami połączonymi odwrotnie równolegle*, *Sterowanie w Energoelektronice i Napędzie Elektrycznym SENE'05*, Łódź, 2005.
- [5] T. Citko, H. Tunia, B. Winiarski.: *Układy rezonansowe w energoelektronice*, Wydawnictwa Politechniki Białostockiej, Białystok 2001.
- [6] M. H. Rashid.: „Power Electronics Handbook” Academic Press, Canada 2001.
- [7] W. Wojtkowski.: *Przekształtnik DC/DC o stałej wysokiej częstotliwości przekształcania energii*. Rozprawa Doktorska, Politechnika Białostocka, Wydział Elektryczny, Białystok, 2004.

Artykuł recenzowany